E1-2001-139

D.V.Naumov, B.A.Popov

A STUDY OF STRANGE PARTICLE PRODUCTION IN ν_μ CHARGED CURRENT INTERACTIONS IN THE **NOMAD** EXPERIMENT

1 INTRODUCTION

The production of strange particles in neutrino interactions is of interest for many reasons. The decays of neutral strange particles such as $K^0_s \to \pi^+\pi^-$, $\Lambda \to p\pi^-$ and $\bar{\Lambda} \to \bar{p}\pi^+$ can be reliably identified in contrast to most other hadrons using the V^0-like signature of their decays. Therefore, they could provide a testing ground for the quark-parton as well as hadronization models. It is noteworthy that all previous investigations of strange particle production by neutrinos have come from bubble chamber experiments [3–22]. No other technique has so far yielded results on this subject. However, previous bubble chamber experiments with (anti)neutrino beams suffered from low statistics of their V^0 samples.

The NOMAD experiment [23] collected a large number of neutrino interactions with a reconstruction quality similar to bubble chamber experiments. The order of magnitude increase in statistics can be used to improve our knowledge of strange particle production in neutrino interactions. In this paper we present our measurements of the integral and differential production rates of neutral strange particles (K^0_s's, Λ's and $\bar{\Lambda}$'s), as well as the yields of $K^{\star\pm}$, $\Sigma^{\star\pm}$, Ξ^-, Σ^0. These results are compared to the predictions of the default NOMAD Monte Carlo simulation program.

The results of the present analysis could be used:

(i) to tune the parameters of the Monte Carlo (MC) simulation program in order to reproduce correctly the production of strange particles in neutrino interactions;
(ii) to take into account the contribution from strange resonances and heavy hyperons decaying into Λ and $\bar{\Lambda}$ for a quantitative theoretical interpretation of the Λ and $\bar{\Lambda}$ polarization measurements in ν_μ CC DIS reported in our previous articles [1,2].

2 EXPERIMENTAL PROCEDURE

2.1 The NOMAD experiment

The main goal of the NOMAD experiment [23] was the search for $\nu_\mu \to \nu_\tau$ oscillations in a wide-band neutrino beam from the CERN SPS. The main characteristics of the beam are given in Table 1. This search uses kinematic criteria to identify ν_τ charged current (CC) interactions [24] and requires a very good quality of event reconstruction similar to that of bubble chamber experiments. This has indeed been achieved by the NOMAD detector, and, moreover, the large data sample collected during four years of data taking (1995-1998) allows for a detailed study of neutrino

interactions. A full data sample from the NOMAD experiment is used in the present analysis. The data are compared to the results of a Monte Carlo simulation based on LEPTO 6.1 [25] and JETSET 7.4 [26] generators for neutrino interactions and on a GEANT [27] based program for the detector response. To define the parton content of the nucleon for the cross-section calculation we have used the GRV-HO parametrization [28] of the parton density functions available in PDFLIB [29]. For the analysis reported below we used a MC sample consisting of 2.3 millions events that passed our selection criteria. This is about a factor of 3 more statistics than in the data sample.

Table 1
The CERN SPS neutrino beam composition (as predicted by the beam simulation program [30]).

Neutrino	Flux		CC interactions in NOMAD	
flavours	$< E_\nu >$ [GeV]	rel.abund.	$< E_\nu >$ [GeV]	rel.abund.
ν_μ	24.0	1	45.5	1
$\bar{\nu}_\mu$	17.0	0.0700	40.9	0.0245
ν_e	36.4	0.0102	57.4	0.0153
$\bar{\nu}_e$	28.1	0.0026	50.5	0.0015

2.2 The NOMAD detector

For a study of strange particle production the tracking capabilities of a detector are of paramount importance. The NOMAD detector (see Fig. 1) is especially well suited to this aim. It consists of an active target of 44 drift chambers, with a total fiducial mass of 2.7 tons, located in a 0.4 Tesla dipole magnetic field. The drift chambers (DC) [31], made of low Z material (mainly Carbon) serve the double role of a (nearly isoscalar) target for neutrino interactions and of the tracking medium. The average density of the drift chamber volume is 0.1 g/cm^3 very close to that of liquid hydrogen. These drift chambers provide an overall efficiency for charged track reconstruction of better than 95% and a momentum resolution which can be parametrized as

$$\frac{\sigma_p}{p} = \frac{0.05}{\sqrt{L}} \oplus \frac{0.008 \cdot p}{\sqrt{L^5}},$$

where the track lenght L is in meters and the track momentum p is in GeV/c. This amounts to approximately 3.5% in the momentum range of interest (less than 10 GeV/c). Reconstructed tracks are used to determine the event topology (the assignment of tracks to vertices), to reconstruct the vertex position and the track

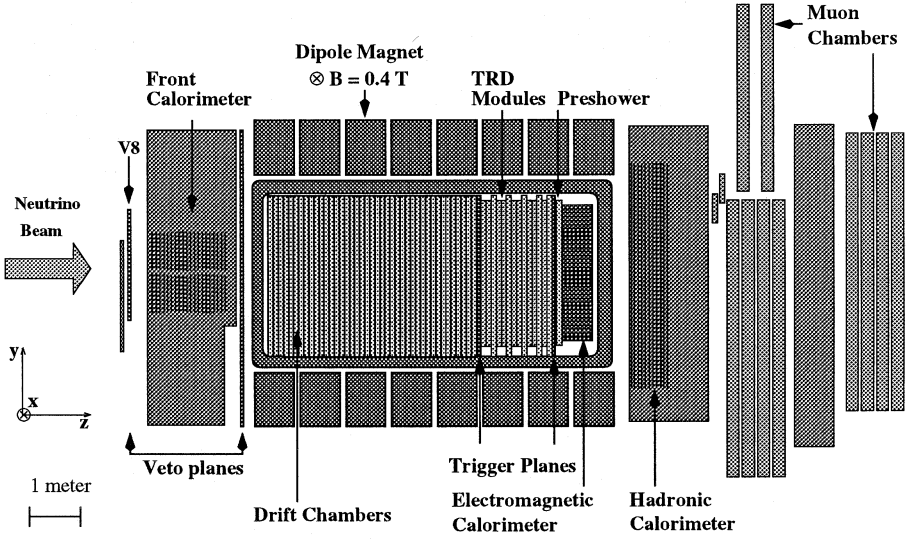

Fig. 1. A sideview of the NOMAD detector.

parameters at each vertex and, finally, to identify the vertex type (primary, secondary, V^0, etc.). A lead-glass electromagnetic calorimeter [32] located downstream of the tracking region provides an energy resolution of $3.2\%/\sqrt{E[\mathrm{GeV}]} \oplus 1\%$ for electromagnetic showers and is essential to measure the total energy flow in neutrino interactions. In addition, an iron absorber and a set of muon chambers located after the electromagnetic calorimeter are used for muon identification, providing a muon detection efficiency of 97% for momenta greater than 5 GeV/c.

The *large statistics of the data* combined with the *good quality of event reconstruction* in the NOMAD detector allows to perform a detailed study of strange particle production in neutrino interactions.

2.3 Event selection and V^0 identification procedure

The NOMAD experiment has collected 1.3×10^6 ν_μ CC events and has observed an unprecedented number of neutral strange particle decays. Such a decay appears in the detector as a V^0-like vertex: two tracks of opposite charge emerging from a common vertex separated from the primary neutrino interaction vertex (see Fig. 2). The V^0-like signature is expected also for photon conversions.

The selection procedure for the ν_μ CC event sample used in this analysis has been described in [1].

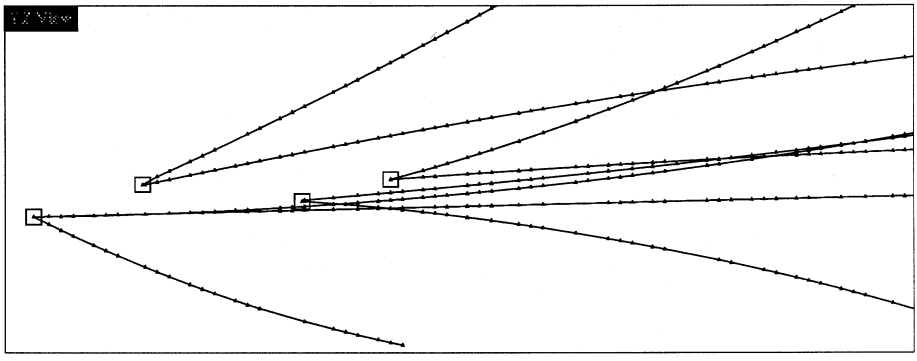

Fig. 2. *A reconstructed data event containing 3 V^0 vertices identified as K^0_s decays by our identification procedure. The scale on this plot is given by the size of the vertex boxes (3×3 cm^2).*

Since the NOMAD detector is unable to distinguish (anti)protons from pions in the momentum range relevant to this analysis, our V^0 identification procedure relies on the kinematic properties of a V^0 decay.

For the V^0 identification a kinematic fit method has been used as described in [1,33]. This fit has been performed for three decay hypotheses: $K^0_s \to \pi^+\pi^-$, $\Lambda \to p\pi^-$, $\bar{\Lambda} \to \bar{p}\pi^+$ and for the hypothesis of a photon conversion $\gamma \to e^+e^-$. The output of the kinematic fits applied to a given V^0 vertex consists of four $\chi^2_{V^0}$. The different regions in the four-dimensional $\chi^2_{V^0}$ space populated by particles identified as K^0_s, Λ and $\bar{\Lambda}$ have been selected. Identified V^0's are of two types:

- *uniquely* identified V^0's, which, in the four-dimensional $\chi^2_{V^0}$ space described above, populate regions corresponding to the decay of different particles;
- *ambiguously* identified V^0's, which populate overlapping kinematic regions in which the decays of different particles are present.

The treatment of ambiguities aims at selecting a given V^0 decay with the highest efficiency and the lowest background contamination from other V^0 types. An optimum compromise between high statistics of the identified V^0 sample and well understood background contamination is the aim of our identification strategy which consists of two steps:

1) we select a subsample of uniquely identified V^0's with high purity (98% for K^0_s's, 97% for Λ's, 90% for $\bar{\Lambda}$'s).
2) then we add a subsample of ambiguously identified V^0's amounting to at most 10% of the total final sample resolving the ambiguities between Λ/K^0_s and $\bar{\Lambda}/K^0_s$ in favour of maximal efficiency and maximal purity of each V^0 category.

Table 2
Efficiency and purity for each selected V^0 category. Numbers of identified neutral strange particles in the data are also shown in the last column.

V^0	ϵ (%)	P (%)	Data
K^0_s	22.1 ± 0.1	97.2 ± 0.1	15074
Λ	16.4 ± 0.1	95.9 ± 0.1	8087
$\bar{\Lambda}$	18.6 ± 0.5	89.7 ± 0.7	649

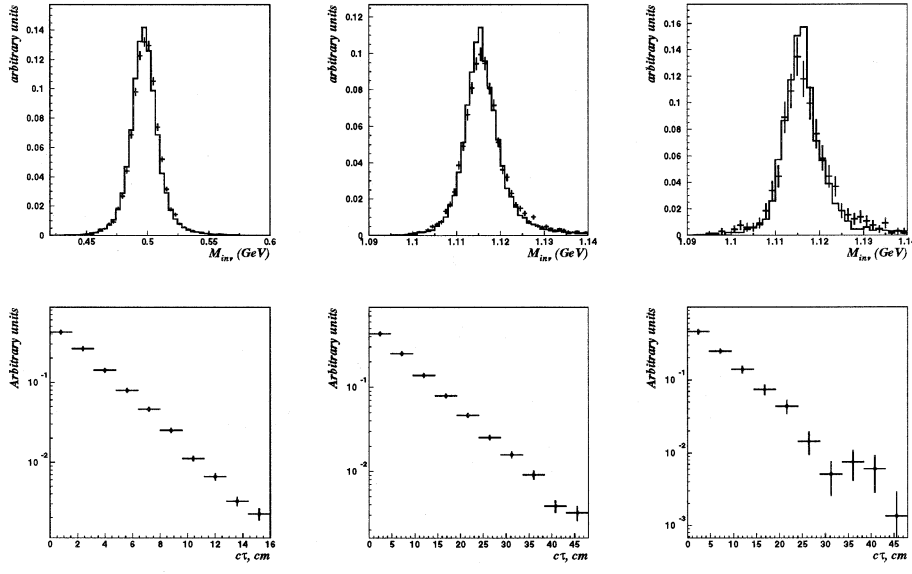

Fig. 3. *Top plots: Invariant mass distributions for identified K^0_s's (left), Λ's (center) and $\bar{\Lambda}$'s (right) in ν_μ CC DIS events. Bottom plots: the corresponding efficiency corrected $c\tau$ distributions for K^0_s's (left), Λ's (center) and $\bar{\Lambda}$'s (right).*

The MC simulation program has been used to study the purity of the K^0_s, Λ and $\bar{\Lambda}$ samples obtained by our selection criteria in ν_μ CC interactions. The corresponding results are reported in Table 2 which also gives the number of neutral strange particles selected in the data by our identification procedure. The total V^0 sample in our data contains 15074 identified K^0_s, 8087 identified Λ and 649 identified $\bar{\Lambda}$ decays, representing significantly larger numbers than in previous (anti)neutrino experiments performed with bubble chambers [3–22]. Fig. 3 shows the invariant mass and $c\tau$ distributions for identified K^0_s's, Λ's and $\bar{\Lambda}$'s. Measured invariant mass and the life time of identified neutral strange particles are in agreement with [34].

In what follows we will present always efficiency corrected distributions.

3 YIELDS OF NEUTRAL STRANGE PARTICLES

We have studied first the production rates of the neutral strange particles (K^0_s, Λ, $\bar{\Lambda}$) in ν_μ CC interactions. The particles can be produced both at the primary vertex and from the secondary interactions of primary produced particles with the detector material. Neutral strange particles produced via resonance or heavier hyperon decays are classified as primary V^0's. We applied a MC correction to the yields of neutral strange particles in the data to extract the yields at the primary vertex.

3.1 Integral yields of neutral strange particles

The measured yield per ν_μ CC interaction for each V^0 type is defined as:

$$T_{V^0} = \xi \cdot \frac{N_{V^0}}{N_{\nu_\mu CC}}, \tag{1}$$

where N_{V^0} is the number of reconstructed and identified V^0's in the number $N_{\nu_\mu CC}$ of reconstructed ν_μ CC events and ξ - is a correction factor calculated as:

$$\xi = \frac{P_{V^0} \times \epsilon_{\nu_\mu CC}}{\epsilon_{V^0} \times Br(V^0 \to h^+h^-)},$$

where $\epsilon_{\nu_\mu CC} = (85.30 \pm 0.02)\%$ is the reconstruction and identification efficiency of ν_μ CC events in the fiducial volume, and ϵ_{V^0} is the global V^0 efficiency which takes into account a contribution from a fraction of particles produced in the fiducial volume, but decaying outside of it. P_{V^0} is the purity of the final V^0 sample, and $Br(V^0 \to h^+h^-)$ is the branching ratio for a given V^0 type decaying into a pair of charged hadrons.

Table 3
Integral yields of primary V^0's in ν_μ CC interactions in both real data and default MC simulation.

V^0 type	$T^{DATA}_{V^0}$ (%)	$T^{MC}_{V^0}$ (%)	$T^{MC}_{V^0}/T^{DATA}_{V^0}$
K^0_s	6.76 ± 0.06	9.50 ± 0.02	1.40 ± 0.01
Λ	5.04 ± 0.06	8.10 ± 0.02	1.61 ± 0.02
$\bar{\Lambda}$	0.37 ± 0.02	0.60 ± 0.01	1.62 ± 0.03

Table 3 shows the overall inclusive production rates for K^0_s, Λ and $\bar{\Lambda}$ in ν_μ CC interactions compared to the MC predictions. As one can easily notice the production

rates in the default MC simulation program is by a factor of $1.4 \div 1.6$ higher than in real data. This could be explained in part by the choice of LEPTO [25] and JETSET [26] parameters in the NOMAD event generator. We have to emphasize that the so-called $s\bar{s}$ suppression factor (PARJ(2) parameter in JETSET) - defined as the ratio of the probability γ_s of producing an $s\bar{s}$ pair to the probability γ_u (γ_d) of producing $u\bar{u}$ ($d\bar{d}$) pair in the fragmentation chain - was set to its default value of 0.3 in the official NOMAD MC production. However, this parameter was measured to be about 0.2 in previous bubble chamber experiments: for example, the values obtained by BEBC [35] in a neutrino beam similar to ours are $0.200 \pm 0.022(stat) \pm 0.010(sys)$ for $\bar{\nu}p$ and $0.207 \pm 0.018(stat) \pm 0.020(sys)$ for νp interactions. Moreover, later results from OPAL (0.245) [36], DELPHI (0.23) [37], E665 (0.2) [38], ZEUS [39] and H1 [40] collaborations support the value closer to 0.2 for this parameter.

Table 4

Numbers of ν_μ CC events with a specified combination of observed neutral strange particle decays for both MC and data. X indicates any hadronic system not containing observed K^0_s, Λ *or* $\bar{\Lambda}$.

Channel	Number of observed events		MC/DATA
	MC	Data	
ΛX	11686	7778	1.50 ± 0.02
$K^0_s X$	18971	14228	1.33 ± 0.01
$\bar{\Lambda} X$	831	594	1.40 ± 0.07
$K^0_s K^0_s X$	485	284	1.7 ± 0.1
$\Lambda K^0_s X$	617	247	2.5 ± 0.2
$\Lambda\bar{\Lambda} X$	98	40	2.5 ± 0.4
$K^0_s \bar{\Lambda} X$	24	15	1.6 ± 0.5
$\Lambda\Lambda X$	19	10	1.9 ± 0.7
$\Lambda K^0_s K^0_s X$	7	2	3.4 ± 2.6
$K^0_s K^0_s K^0_s X$	2	4	0.6 ± 0.4

A new version of the NOMAD event generator has been tuned to better reproduce the fragmentation process and contains PARJ(2)=0.21. However, the problem of the wrong description of neutral strange particle production in our MC is more complicated. As a confirmation in Table 4 we give the observed numbers of ν_μ CC events for 10 specific multi-V^0 channels in the data compared to the MC predictions. The number of MC events in Table 4 is renormalized to the same number of ν_μ CC events as in the data. From this comparison one can conclude that it is not possible

to rescale just a single parameter (the $s\bar{s}$ suppression factor) in order to describe the neutral strange particle production observed in the data. The discrepancy is rather due to a combination of several parameters which describe the probabilities that $s(\bar{s})$-quark appears as a meson/baryon(antibaryon), the probabilities that a strange meson/baryon(antibaryon) will appear electrically neutral, etc. A tuning of the JETSET parameters to reproduce the yields of neutral strange particles observed in the NOMAD data is a subject of an independent analysis currently in progress.

The integral yields reported in Table 3 could be compared to previous measurements summarized in Table 5. The K^0_s rates from Table 3 have been transformed into $K^0 (= K^0 + \bar{K^0})$ rates multiplying by a factor of 2.

Let us note the discrepancies between the integral yields reported by previous experiments. These discrepancies could be either due to some additional kinematical cuts which are left out of tables summarizing V^0 rates from different experiments (cuts on the muon momentum, hadronic energy, W^2, etc.) or due to a contribution from non-prompt production of neutral strange particles (V^0's originating from secondary interactions). Unlike most other experiments our data sample has no explicit cuts on kinematic variables. For the purspose of the comparison with the rates reported by previous experiments we have also recalculated the integral overall yields taking into account contributions from both primary and secondary V^0's. These results are given in Table 3 and denoted by a star ($\star$). Our overall yields are consistent with the results of the ν-Ne experiment [18] performed in a similar neutrino beam. However, our primary yields of K^0_s's and Λ's are $30 \div 35\%$ lower and $\sim 20\%$ lower for $\bar{\Lambda}$'s.

In the next section we present differential production rates of neutral strange particles as functions of relevant kinematic variables.

3.2 Differential production rates of neutral strange particles

To investigate neutral strange particle production mechanisms we have measured the average K^0_s, Λ and $\bar{\Lambda}$ multiplicities as functions of the neutrino energy E_ν, the invariant square of the hadronic system's effective mass W^2, the invariant square of the four-momentum transfer from the neutrino to the muon Q^2, and the Bjorken scaling variable x_{Bj}.

The differential production rates for K^0_s's, Λ's and $\bar{\Lambda}$'s are shown in Fig. 4. The differential Λ production rate shows a behaviour which is almost independent of E_ν, W^2, Q^2 after a sharp initial rise. It drops at large values of x_{Bj}. On the contrary, the production of K^0_s rises steadily with E_ν and W^2, it reaches a plateau at large Q^2 and falls with increasing x_{Bj}. Similar observations have been made by previous experiments, but with larger statistical uncertainties. The differential $\bar{\Lambda}$ production

Table 5
Inclusive production rates of neutral strange particles in $\nu_\mu N$ CC interactions measured in this analysis and in previous bubble chamber experiments. N_K, N_Λ and $N_{\bar{\Lambda}}$ are the observed numbers of K^0_s's, Λ's and $\bar{\Lambda}$'s, respectively, while the rates are fully corrected (the errors on the rates are taken from the original publications). K^0 stands for $K^0 + \bar{K}^0$.

Reaction [Ref]	$< E_\nu >$ (GeV)	$N_{K^0_s}$	K^0 rate (%)	N_Λ	Λ rate (%)	$N_{\bar{\Lambda}}$	$\bar{\Lambda}$ rate (%)
NOMAD	46	15075	13.52 ± 0.12	8087	5.04 ± 0.06	649	0.37 ± 0.02
NOMAD*			18.22 ± 0.16		6.66 ± 0.08		0.45 ± 0.02
ν - Ne [18]	46	2279	16.8 ± 1.2	1843	6.5 ± 0.5	93	0.46 ± 0.08
ν - p [21]	51	831	19.0 ± 0.9	491	5.2 ± 0.3	27	0.34 ± 0.07
ν - Ne [22]	150	502	40.8 ± 4.8	285	12.7 ± 1.4	27	1.5 ± 0.5
ν - p [12]	43	359	17.5 ± 0.9	180	4.5 ± 0.4	13	0.3 ± 0.1
ν - Ne [13]	103	203	23.0 ± 1.7	98	5.7 ± 0.7		
ν - n [14]	62	234	20.8 ± 1.6	157	7.1 ± 0.7		
ν - p [14]	62	154	17.7 ± 1.6	77	4.3 ± 0.6		
ν - n [16]	62		20.5 ± 1.1		6.6 ± 0.7		
ν - p [16]	62		17.4 ± 1.2		4.4 ± 0.5		
ν - p [11]	$\sim$45	23	15 ± 4				
ν - p [15]	$\sim$50				7.0 ± 0.8		
ν - n [15]	$\sim$50				7.0 ± 1.2		

rates are measured for the first time in a neutrino experiment. In general they show a behaviour similar to the K^0_s one. However, as expected, clear W^2 and E_ν thresholds are present in the $\bar{\Lambda}$ production.

The ratios of differential production rates for K^0_s/Λ and $\bar{\Lambda}/\Lambda$ are presented in Fig. 5.

3.3 Comparison with LUND model predictions

The measured differential distributions of events containing identified K^0_s, Λ, $\bar{\Lambda}$ particles in data are compared to the corresponding MC distributions in Figs. 6, 7, 8.

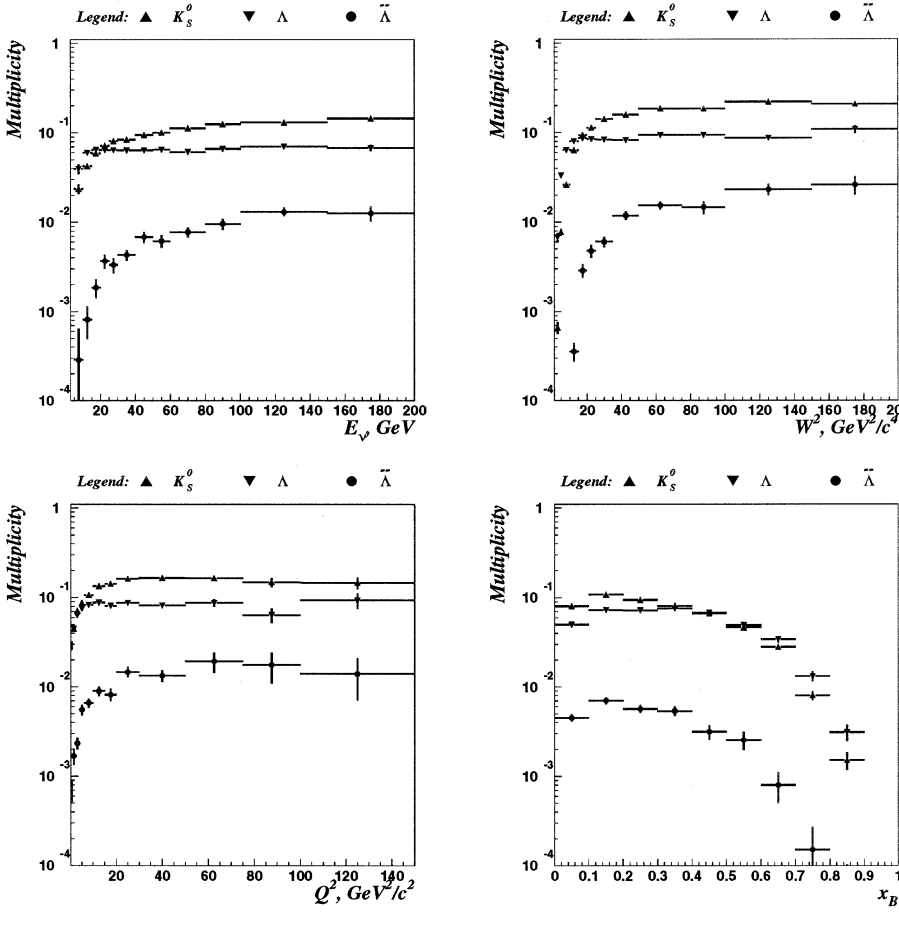

Fig. 4. *Differential production rates in the real data for* K_s^0*'s,* Λ*'s and* $\bar{\Lambda}$*'s as a function of the incoming neutrino energy* E_ν*,* W^2*,* Q^2 *and* x_{Bj}*.*

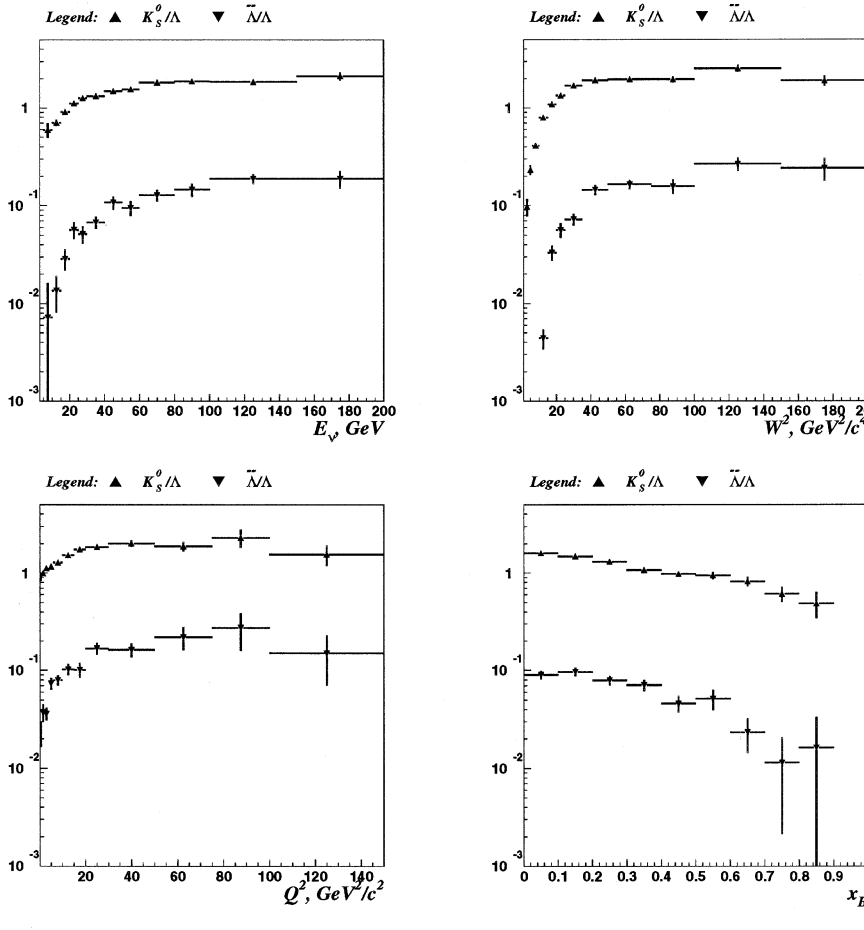

Fig. 5. *Ratios of differential production rates for* K^0_S/Λ *and* $\bar{\Lambda}/\Lambda$ *in the real data as a function of the incoming neutrino energy* E_ν, W^2, Q^2 *and* x_{Bj}.

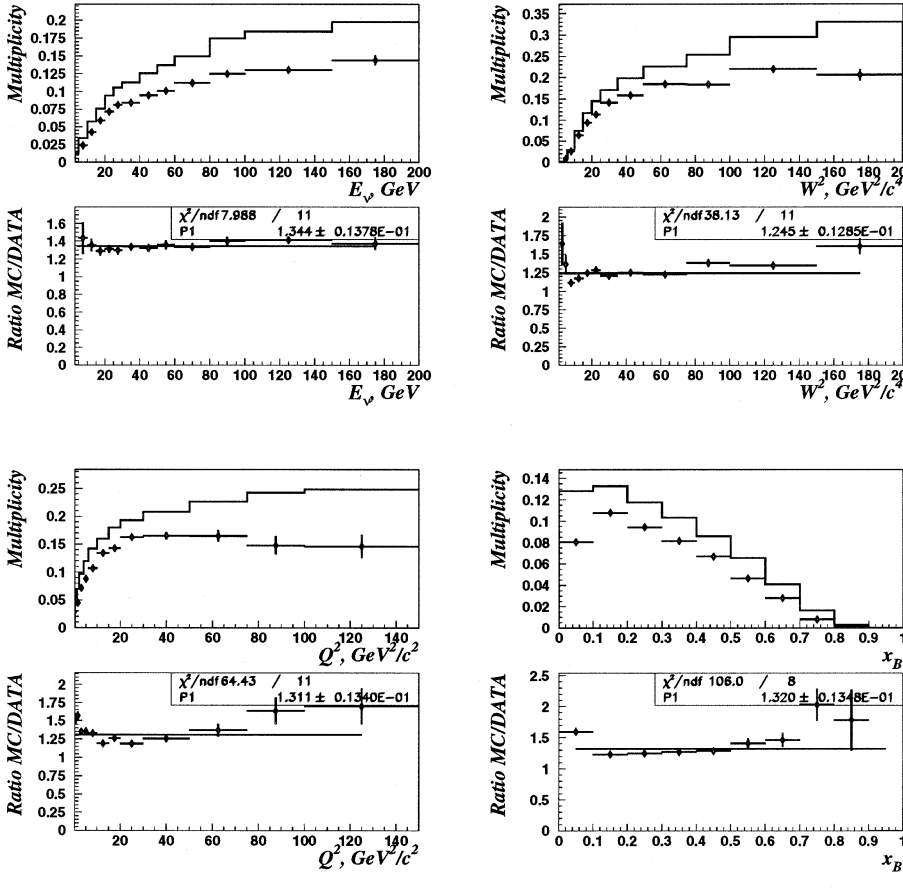

Fig. 6. *Differential production rates in the default MC (histogram) and real data (points with error bars) for* K^0_s*'s as a function of the incoming neutrino energy* E_ν*,* W^2*,* Q^2 *and* x_{Bj}*. The MC/Data ratios are also shown.*

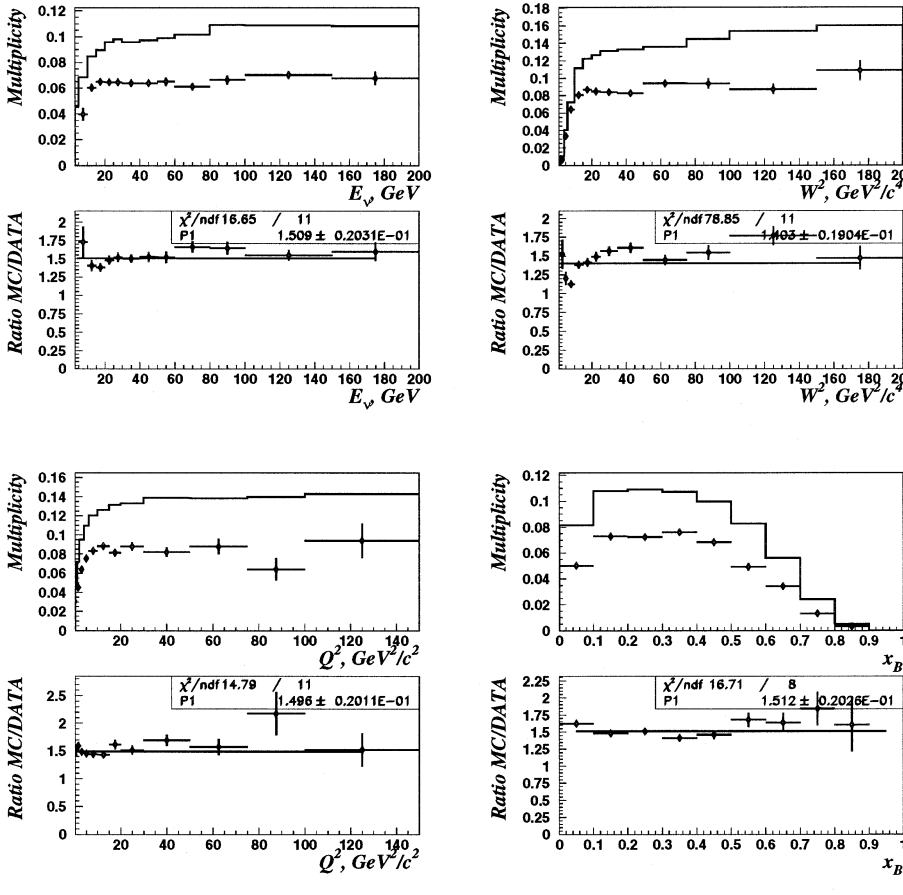

Fig. 7. *Differential production rates in the default MC (histogram) and real data (points with error bars) for Λ's as a function of the incoming neutrino energy E_ν, W^2, Q^2 and x_{Bj}. The MC/Data ratios are also shown.*

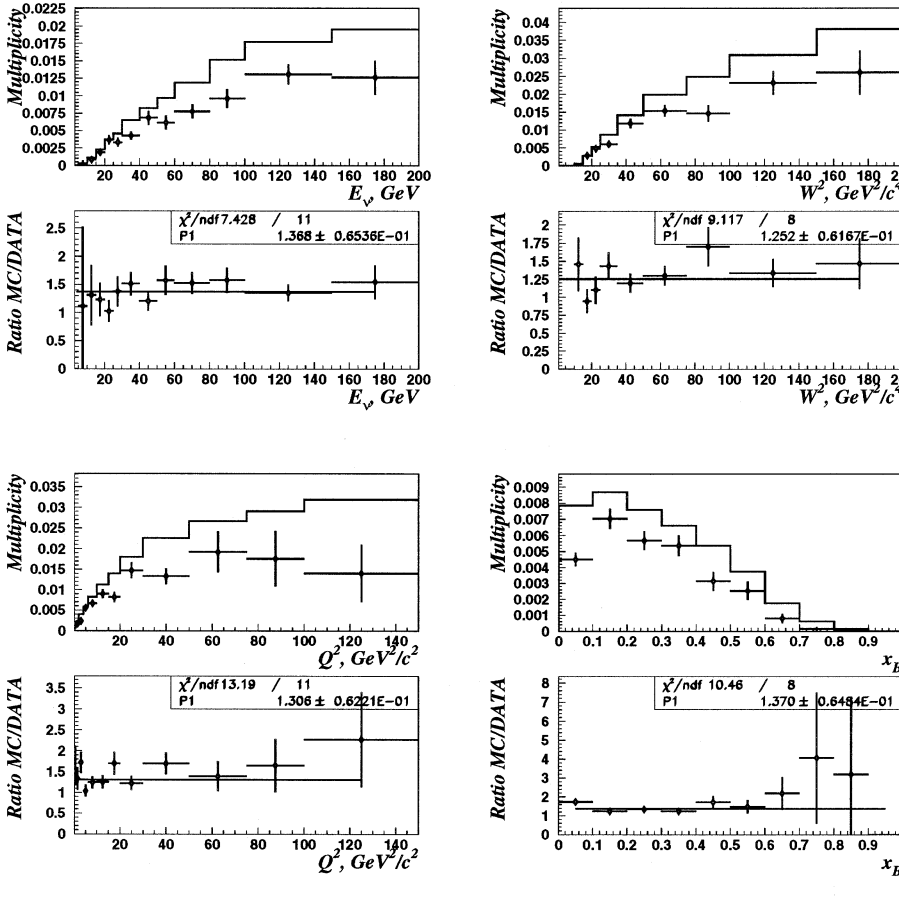

Fig. 8. *Differential production rates in the default MC (histogram) and real data (points with error bars) for $\bar{\Lambda}$'s as a function of the incoming neutrino energy E_ν, W^2, Q^2 and x_{Bj}. The MC/Data ratios are also shown.*

4 PRODUCTION PROPERTIES

We have also performed a detailed analysis of kinematic quantities describing the behaviour of neutral strange particles (K^0_s, Λ and $\bar{\Lambda}$) inside the hadronic jet. This study allows an investigation of the dynamics of fragmentation. The differences in the production properties of K^0_s's, Λ's and $\bar{\Lambda}$'s are seen most clearly here. The following distributions could be of interest: $x_F = 2p^*_L/W$ (Feynman-x is the longitudinal momentum fraction in the hadronic center of mass system), the transverse momentum squared, p^2_T, of a particle with respect to the current (hadronic jet) direction, the fraction $z = E_{lab}(V^0)/E_{lab}(\text{all hadrons})$ of the total hadronic energy carried away by the neutral strange particle in the laboratory system.

There are different mechanisms responsible for K^0_s, Λ and $\bar{\Lambda}$ production in νN CC DIS process which are expected to give different x_F and z distributions of these particles.

- x_F distribution of K^0_s mesons produced promptly in $W^+d \to u$ process that requires at least two quark-antiquark pairs to be created ($d\bar{d}$ and $s\bar{s}$) is expected to be central. A contribution from heavier strange particle decays (mainly from K^{*+}) produced from the struck u quark fragmentation can result in a forward x_F distribution of K^0_s mesons. Also K^0_s mesons from a fragmentation of the struck (anti)quark in $W^+d \to c \to s$ and $W^+\bar{u} \to \bar{d}$ processes are expected to be produced in the forward x_F region and to carry a larger fraction of the jet energy.
- Λ hyperons can be produced from the fragmentation of the nucleon di-quark remnant promptly and via decays of heavier strange baryons at $x_F < 0$. Λ hyperons can be produced also at $x_F > 0$ from the u quark fragmentation.
- A production of $\bar{\Lambda}$ hyperons in the neutrino scattering on a valence quark requires three quark-antiquark pairs to be created ($u\bar{u}$, $d\bar{d}$ and $s\bar{s}$) that is expected to give a central x_F distribution. There could also be a contribution from the struck sea antiquark fragmentation into $\bar{\Lambda}$ hyperon (in the $W^+\bar{u} \to \bar{d} \to \bar{\Lambda}$ process) which can produce these baryons in the forward x_F region.

4.1 x_F distributions

The efficiency corrected x_F distributions observed in real data for neutral strange particles are shown in Fig. 9. The x_F distributions indicate that Λ's are produced mainly in the target fragmentation region, while K^0_s's are peaked in the central region with an asymmetry in the forward direction as expected for particles produced in the current fragmentation region. $\bar{\Lambda}$'s are produced in the central x_F region ($|x_F| < 0.5$). One way to quantify differences in the x_F distributions is to define an asymmetry parameter $A = (N_F - N_B)/(N_F + N_B)$, where N_F and N_B are the numbers of

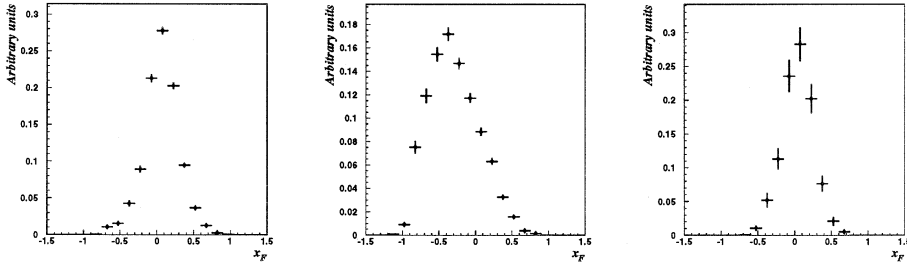

Fig. 9. *Efficiency corrected x_F distributions for K^0_s (left), Λ (centre) and $\bar{\Lambda}$ (right).*

particles going forward and backward, respectively, in the hadronic center of mass. The asymmetry parameters A and mean values of x_F in both data and MC can be found in Table 6.

Table 6
Asymmetry parameters A and mean values of x_F distributions for K^0_s, Λ, $\bar{\Lambda}$ in both MC and data.

V^0	MC		DATA	
	$\langle x_F \rangle$	A	$\langle x_F \rangle$	A
K^0_s	0.055 ± 0.001	0.152 ± 0.002	0.064 ± 0.001	0.256 ± 0.004
Λ	-0.296 ± 0.001	-0.649 ± 0.002	-0.295 ± 0.002	-0.589 ± 0.004
$\bar{\Lambda}$	0.006 ± 0.002	-0.03 ± 0.01	0.04 ± 0.004	0.18 ± 0.02

4.2 z distributions

Efficiency corrected z distributions for K^0_s (left), Λ (centre) and $\bar{\Lambda}$ (right) are shown in Fig. 10. A turn-over at small values of z can be seen for $\bar{\Lambda}$ hyperons, while for K^0_s and Λ this effect is less evident. The effect of turn-over at small values of z for K^0_s and Λ was observed in some of the previous neutrino experiments [9,12,14,19] and was not observed in others [11,13]. It is important to note that uncorrected z distributions show such a turn-over for all V^0's in our experiment as well due to less efficient reconstruction of particles at small momenta.

Below we separately study z distributions of neutral strange particles produced at $x_F < 0$ (see § 4.2.1) and at $x_F > 0$ (see § 4.2.2).

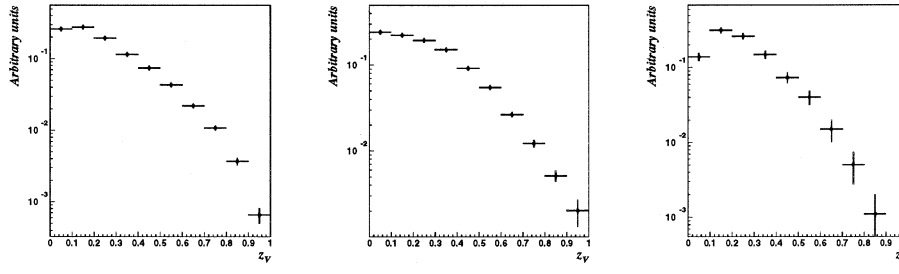

Fig. 10. *Efficiency corrected z distributions for* K^0_s *(left),* Λ *(centre) and* $\bar{\Lambda}$ *(right).*

Table 7
Mean values of z distributions for K^0_s, Λ, $\bar{\Lambda}$ *measured for the full sample and for* $x_F < 0$ *and* $x_F > 0$ *selections in both MC and data.*

V^0		full sample	$x_F < 0$	$x_F > 0$
K^0_s	MC	0.218 ± 0.001	0.092 ± 0.001	0.312 ± 0.001
	DATA	0.226 ± 0.001	0.105 ± 0.001	0.299 ± 0.001
Λ	MC	0.227 ± 0.001	0.179 ± 0.001	0.462 ± 0.003
	DATA	0.250 ± 0.002	0.206 ± 0.001	0.434 ± 0.005
$\bar{\Lambda}$	MC	0.215 ± 0.003	0.139 ± 0.002	0.296 ± 0.004
	DATA	0.242 ± 0.005	0.147 ± 0.005	0.308 ± 0.008

4.2.1 z distributions in the target fragmentation region

The efficiency corrected z distributions of K^0_s, Λ and $\bar{\Lambda}$ measured in the target fragmentation region are shown in Fig. 11. One can see that the z distribution of K^0_s mesons has a maximum at $z \to 0$ and decreases faster at larger z (compared with Fig. 10) and that the K^0_s mesons produced in the target fragmentation region carry in general a small fraction of the hadronic jet energy. Λ hyperons are believed to be produced mostly from the remnant di-quark fragmentation and the shape of z distribution is similar to that displayed in Fig. 10. The turn-over in z distribution is observed for $\bar{\Lambda}$ hyperons produced in the target fragmentation region.

4.2.2 z distributions in the current fragmentation region

The efficiency corrected z distributions of K^0_s, Λ and $\bar{\Lambda}$ measured in the current fragmentation region are shown in Fig. 12. This kinematical region is interesting because of the u or $\bar{d}$ (anti)quark fragmentation into Λ or $\bar{\Lambda}$ hyperons. All three

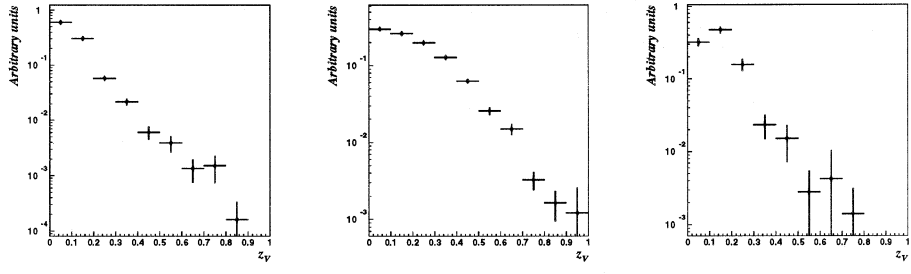

Fig. 11. *Efficiency corrected z distributions for* $x_F < 0$ *for* K^0_s *(left),* Λ *(centre) and* $\bar{\Lambda}$ *(right).*

z distributions show similar behaviour but with different mean values of z. The z distribution of Λ hyperons at $x_F > 0$ is drastically different from that in the target fragmentation region. This is an evidence for the struck u quark fragmentation into Λ hyperon. In fact, z distribution of Λ in the current fragmentation region is a measure of the $D_u^{\Lambda}(z)$ fragmentation function with a unitary normalization. The z distribution of $\bar{\Lambda}$ hyperons is sensitive to the $D_{\bar{d}}^{\bar{\Lambda}}(z)$ fragmentation function with a possible contribution from the $D_u^{\bar{\Lambda}}(z)$ process. One can see that it is slightly harder than the one in the target fragmentation region.

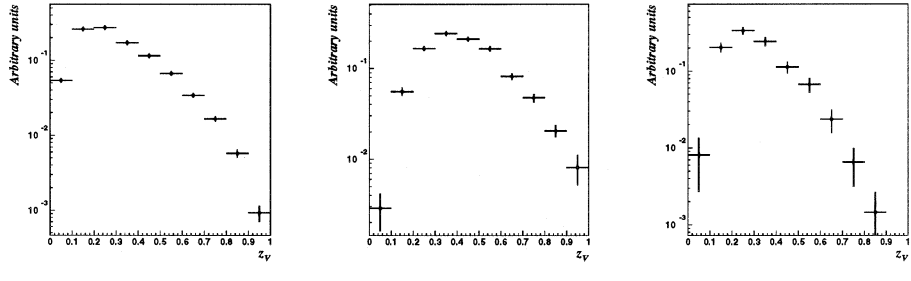

Fig. 12. *Efficiency corrected z distributions for* $x_F > 0$ *for* K^0_s *(left),* Λ *(centre) and* $\bar{\Lambda}$ *(right).*

4.3 p_T^2 *distributions*

The efficiency corrected p_T^2 distributions of K^0_s, Λ and $\bar{\Lambda}$ in the data are shown in Fig. 13.

The p_T^2 distributions of neutral strange particles show an exponential behaviour of the form $a \cdot exp(-B \cdot p_T^2)$ in the region $0 < p_T^2(GeV^2/c^4) < 0.5$. We measured the

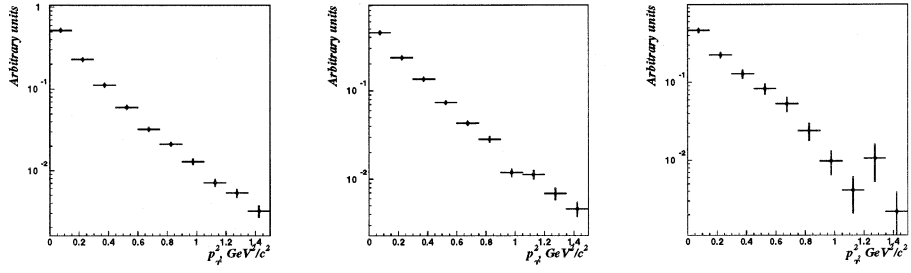

Fig. 13. *Efficiency corrected p_T^2 distributions for K_s^0 (left), Λ (centre) and $\bar{\Lambda}$ (right).*

slope parameter for each V^0 category separately in kinematic regions with no cut on x_F, and for $x_F < 0$ and $x_F > 0$ selections. The slope parameter B after the fit for K_s^0, Λ, $\bar{\Lambda}$ in both MC and data can be found in Table 8. The values of the slope parameter found in different x_F regions are consistent with each other, except for $\bar{\Lambda}$ hyperons.

Table 8

The slope parameter $B(GeV/c)^{-2}$ of p_T^2 distribution for K_s^0, Λ, $\bar{\Lambda}$ measured separately for the full sample and for $x_F < 0$ and $x_F > 0$ selections in both MC and data.

V^0	MC			DATA		
	full sample	$x_F < 0$	$x_F > 0$	full sample	$x_F < 0$	$x_F > 0$
K_s^0	5.72 ± 0.03	5.61 ± 0.04	5.79 ± 0.03	5.21 ± 0.10	5.40 ± 0.21	5.15 ± 0.11
Λ	4.35 ± 0.03	4.30 ± 0.03	4.58 ± 0.06	4.12 ± 0.13	4.18 ± 0.15	4.07 ± 0.27
$\bar{\Lambda}$	3.89 ± 0.10	4.10 ± 0.13	3.70 ± 0.14	4.42 ± 0.47	6.59 ± 0.74	3.30 ± 0.64

5 STRANGE RESONANCES AND HEAVIER HYPERONS

A study of the production of resonances and heavy hyperons [1] is of great importance for both tuning of the LUND model predictions in the MC simulation program and for the theoretical interpretation of the Λ and $\bar{\Lambda}$ polarization measurements reported in our previous articles [1,2]. It is essential because Λ's originating from the decays $\Sigma^\star \to \Lambda\pi$, $\Sigma^0 \to \Lambda\gamma$ and $\Xi \to \Lambda\pi$ have the polarization inherited from the polarization of the parent particles and this polarization is different from the one of the directly produced Λ's. Information about (Σ^0, Ξ) ($\frac{1}{2}^+$), ($\Sigma^\star$, $\Xi^\star$) ($\frac{3}{2}^+$), and $K^\star$ (1^-) yields can be obtained via an analysis of their decays into channels with identified neutral strange particles [33,41].

Previous bubble chamber experiments with (anti)neutrino beams suffered from a lack of statistics. For example, BEBC [21] reported the observation of 149 ± 29 of $K^{\star+}$, 42 ± 19 of $K^{\star-}$, 134 ± 19 of $\Sigma^{\star+}$ and < 10 of $\Sigma^{\star-}$ in $\nu_\mu p$ CC interactions, while Fermilab 15-ft bubble chamber [18] found 94 ± 25 of Σ^0 and 4 Ξ^- in $\nu_\mu Ne$ CC events.

5.1 A procedure for the signal extraction

Our aim was to extract a fraction of neutral strange particles which are decay products of resonances and heavier hyperons from the corresponding invariant mass (M_{res}) distributions. To construct the M_{res} distribution we combine the neutral strange particle with all possible charged tracks (of appropriate sign) emerging from the primary vertex except for those identified as muons or electrons. We have also studied the (Λ γ) combinations, where photons are identified as conversions in the detector fiducial volume via our V^0 identification procedure. The resulting distributions are fitted by a theoretical function describing both the combinatorial background and the resonance signal.

The combinatorial background (BG) can be approximated by any function of the form:

$$BG = P_n(M_{res} - M_{threshold}) \cdot Tail(M_{res}), \tag{2}$$

where $P_n(M_{res} - M_{threshold})$ is a polynomial of the order n vanishing at $M_{res} = M_{threshold}$ ($M_{threshold}$ is the mass threshold, e.g. $M_{threshold} = M_{V^0} + m_\pi$), and $Tail(M_{res})$ is any function vanishing at $M_{res} \to \infty$ faster than P_n increases.

[1] In this section notation Λ applies to both Λ and $\bar{\Lambda}$ under the assumption that particles are replaced by existing antiparticles.

We have chosen the following BG parametrization:

$$BG = a_1 \Delta^{a_2} e^{-(a_3\Delta + a_4\Delta^2)}, \tag{3}$$

where $\Delta = M_{res} - M_{threshold}$.

For a resonance signal the Breit-Wigner (BW) function [42] is used:

$$BW(M_{res}) = \frac{\Gamma_0}{(M_{res}^2 - M_0^2)^2 + M_0^2\Gamma_0^2} \frac{M_0}{q_0}, \tag{4}$$

where M_0, Γ_0, q_0 are the resonance mass, width, and the momentum of the decay product in the resonance rest frame.

Finally, the invariant mass distributions are fitted with:

$$\frac{dN}{dm} = (1 + a_5 BW(M_{res}))BG(\Delta), \tag{5}$$

for all combinations except $(\Lambda\ \pi^-)$, where two peaks due to $\Sigma^{*-} \to \Lambda\pi^-$ and $\Xi^- \to \Lambda\pi^-$ decays are expected. This invariant mass distribution is fitted with

$$\frac{dN}{dm} = (1 + a_5 BW_{\Sigma^{*-}}(M_{res}) + a_6 BW_{\Xi^-}(M_{res}))BG(\Delta), \tag{6}$$

where for the width Γ_0 in the Breit-Wigner function corresponding to the Ξ^- decay a reconstructed resolution on the invariant mass is used.

In the above formulae a_1 to a_6 are free parameters of the fit.

5.1.1 Getting the number of signal events with the error

After the fit one can estimate the number of resonance signal events as:

$$N_s = 1/h \cdot \int_{m_1}^{m_2} a_5 BW(m)BG(m - M_{threshold})dm, \tag{7}$$

where h is the bin-width and m_1, m_2 are the (left,right) bounds of the fitted histogram.

Since this procedure is not a direct measurement of the signal, the errors Δa_i on the parameters a_i are translated into the error on N_s as (neglecting possible correlations):

$$\sigma^2 = \sum_i \left(\frac{\partial}{\partial a_i} \int_{m_1}^{m_2} dm \frac{dN(m|\mathbf{a})}{dm} \right)^2 (\Delta a_i)^2, \tag{8}$$

where $\frac{dN}{dm}$ is the fitting function in Eq. 5 or Eq. 6 which depends on the vector of parameters $\mathbf{a} = (a_1, ..., a_6)$.

5.1.2 Another approach to the signal extraction

A different method to extract the number of signal events with the error which takes into account possible correlations with the other free parameters has been used. Namely, we have fitted the invariant mass distributions by:

$$\frac{dN}{dm} = BG'(\Delta) + a'_5 BW'(M_{res}), \tag{9}$$

where the Breit-Wigner function $BW'(M_{res})$ has been normalized to the unit area.

Similarly,

$$\frac{dN}{dm} = BG'(\Delta) + a'_5 BW'_{\Sigma^{*-}}(M_{res}) + a'_6 BW'_{\Xi^-}(M_{res}) \tag{10}$$

In such a case using the HESSE and MINOS procedures of MINUIT [43], the parameter $a'_5(a'_6)$ gives the number of signal events with the corresponding error which takes into account possible correlations between different parameters.

The results obtained using these two approaches were found to be similar. In what follows we present our results using the second method.

The yields of resonances and heavy hyperons have been studied in different kinematic regions and for neutrino interactions on different target nucleons.

5.1.3 The type of target nucleon

In NOMAD it is possible to separate neutrino interactions on neutron and proton imposing a cut on the sum of charges (Q_{tot}) of all the outgoing tracks at the primary neutrino interaction vertex.

We select νp events requiring $Q_{tot} \geq 1$. According to the MC simulation, the corresponding sample of proton-like events contains about 76% of true νp interactions.

The νn events are selected by the requirement $Q_{tot} \leq 0$. The purity of the corresponding neutron-like sample is about 85%.

5.1.4 Fragmentation region

Since different production mechanisms of hadrons are expected in the target and in the current fragmentation regions it is important to study separately the yields of resonances and heavy hyperons at $x_F < 0$ and $x_F > 0$. Also such a study is necessary for a correct theoretical interpretation of $\Lambda(\bar{\Lambda})$ polarization measurements reported in our previous papers [1,2].

5.2 Studied resonances and heavier hyperons

In what follows we present the number of resonance and heavier hyperon decays found in the data. We give also the MC prediction, denoted as MC(pred.), for the number of studied heavy strange particles and the same quantity extracted from the MC sample using our procedure, denoted as MC(meas.), both of them normalized to the same number of ν_μ CC events as in the data.

The following resonances and heavier hyperons have been studied in the present analysis.

5.2.1 $K^{\star\pm}$

The fitted $(K^0_s\ \pi^\pm)$ invariant mass distributions are shown in Fig. 14 for both Monte Carlo and data samples. A detailed information on the number of extracted $K^{\star\pm}$ events and the $K^{\star\pm}/K^0_s$ ratio is given in Tables 9 and 10. For the $K^{\star\pm}$ mass and width we have used 891.66 MeV and 50.8 MeV. The q_0 value is 291 MeV [34].

It is interesting to note a more abundant $K^{\star+}$ production in ν_μN DIS compared to $K^{\star-}$ one. This can be explained by the fact that the struck quark u could be fragmenting directly into a $K^{\star+}$, while both $\bar{u}$ and s quarks needed to produce a $K^{\star-}$ meson have to be created in the fragmentation process.

One can see that there is an important difference between $K^{\star\pm}$ yields in the default MC simulation and the NOMAD data (up to a factor of 2).

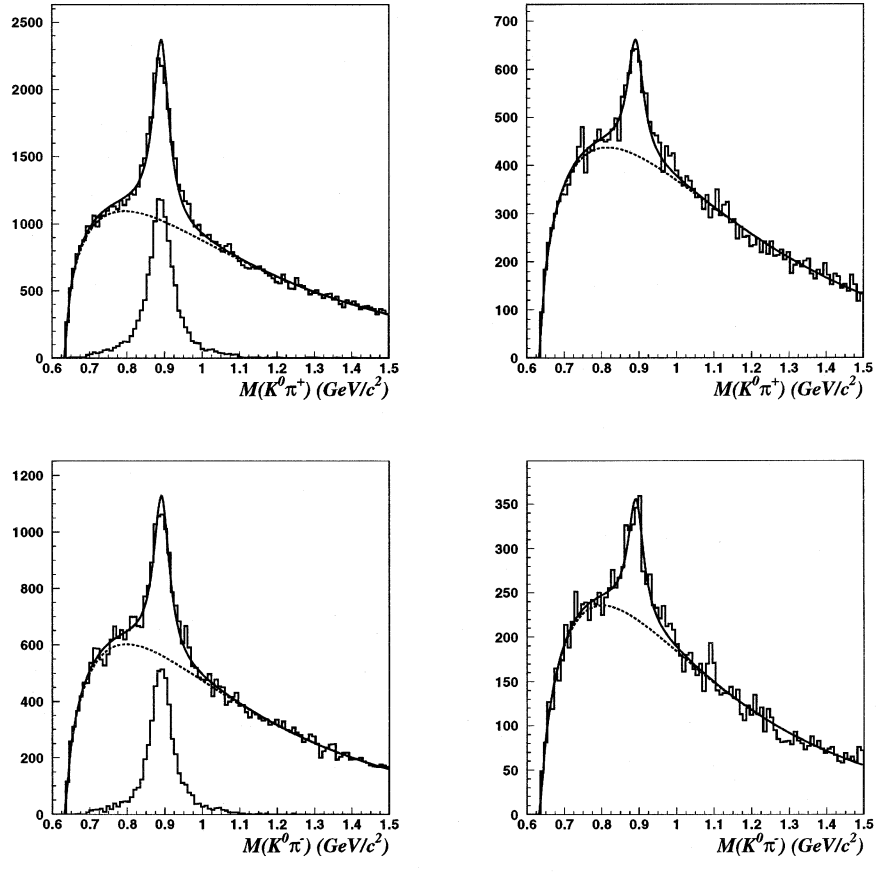

Fig. 14. $K^0_s\pi^+$ *(top) and* $K^0_s\pi^-$ *(bottom) invariant mass distributions for both MC (left) and data (right). The MC plots show the expected signal peaks.*

5.2.2 $\Sigma^{\star\pm}$

The fitted invariant mass distributions for ($\Lambda\ \pi^\pm$) combinations in both Monte Carlo and data samples are shown in Fig. 15. A detailed summary of the number of extracted $\Sigma^{\star\pm}$ events and the $\Sigma^{\star\pm}/\Lambda$ ratio is given in Tables 11 and 12. For the $\Sigma^{\star\pm}$ mass and width we have taken the values from [34]: m($\Sigma^{\star+}$)=1382.8 MeV, $\Gamma(\Sigma^{\star+})$=35.8 MeV, m($\Sigma^{\star-}$)=1387.2 MeV, $\Gamma(\Sigma^{\star-})$=39.4 MeV. The q_0 value is 208 MeV.

A striking difference between $\Sigma^{\star\pm}$ yields in the default MC simulation and the

Table 9
$K^{\star+} \to K^0_s \pi^+$ *summary*

$N(K^{\star+})$	full sample	K^0_s fragmentation region		type of target nucleon	
		$x_F < 0$	$x_F > 0$	νp	νn
DATA	2036 ± 121	315 ± 56	1731 ± 108	1006 ± 87	1032 ± 84
MC(meas.)	5373 ± 104	726 ± 47	4744 ± 93	1963 ± 67	3516 ± 80
MC(pred.)	5953	886	5067	2206	3748
$N(K^{\star+})/N(K^0_s)$					
DATA (%)	13.5 ± 0.8	9.7 ± 1.7	14.6 ± 0.9	15.7 ± 1.4	11.9 ± 1.0
MC (%)	27.3 ± 0.5	14.5 ± 0.9	31.6 ± 0.6	29.0 ± 1.0	26.5 ± 0.6

Table 10
$K^{\star-} \to K^0_s \pi^-$ *summary*

$N(K^{\star-})$	full sample	K^0_s fragmentation region		type of target nucleon	
		$x_F < 0$	$x_F > 0$	νp	νn
DATA	1146 ± 89	288 ± 44	865 ± 78	377 ± 52	775 ± 73
MC(meas.)	2304 ± 74	639 ± 38	1664 ± 63	729 ± 39	1576 ± 63
MC(pred.)	2467	723	1743	734	1733
$N(K^{\star-})/N(K^0_s)$					
DATA (%)	7.6 ± 0.6	8.9 ± 1.3	7.3 ± 0.7	5.9 ± 0.8	8.9 ± 0.8
MC (%)	11.5 ± 0.4	12.7 ± 0.8	11.1 ± 0.4	10.8 ± 0.6	11.9 ± 0.5

NOMAD data (a factor of about 3 or even larger) is observed.

5.2.3 Ξ^-

The bottom plots in Fig. 15 show evidence for the $\Xi^- \to \Lambda\pi^-$ decays. A detailed summary of the number of extracted Ξ^- events and the Ξ^-/Λ ratio is given in Table 13. For the Ξ^- mass we have used 1321.32 MeV [34], for the width the experimental resolution of 10 MeV has been taken. The q_0 value is 139 MeV.

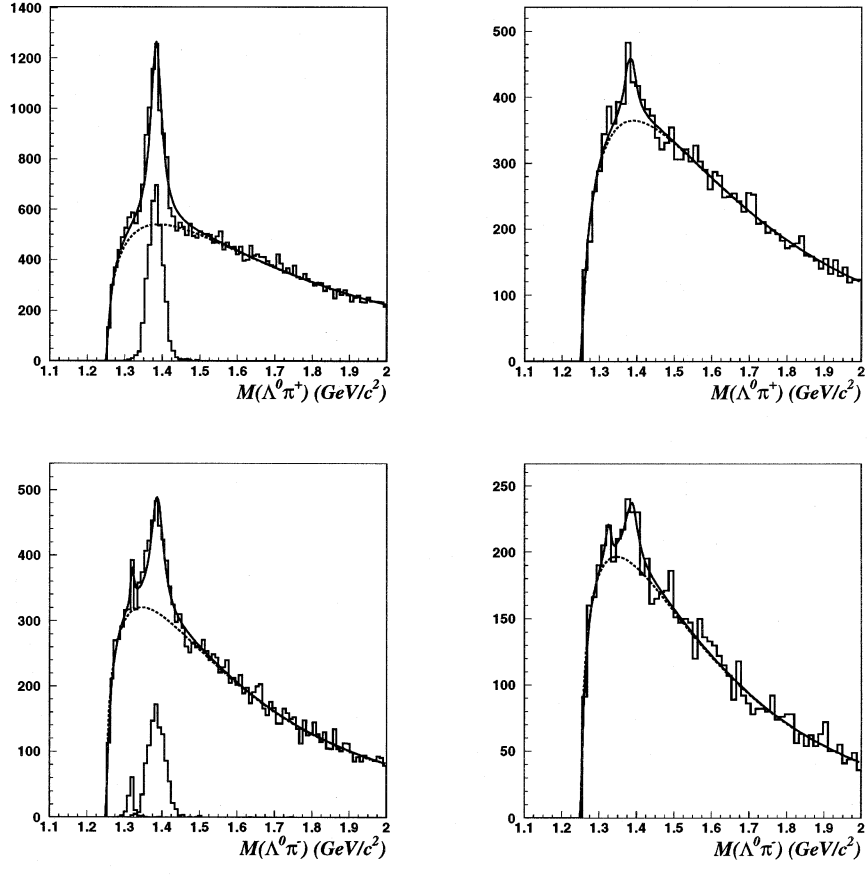

Fig. 15. $\Lambda\pi^+$ *(top) and* $\Lambda\pi^-$ *(bottom) invariant mass distributions for both MC (left) and data (right). The MC plots show the expected signal peaks.*

5.2.4 Σ^0

Fig. 16 shows the fitted invariant mass distributions for $(\Lambda\ \gamma)$ combinations in both Monte Carlo and data samples. The corresponding photons have been reconstructed as conversions in the DC fiducial volume and identified by our V^0 identification procedure. To illustrate the quality of the photon reconstruction we show also the $(\gamma\gamma)$ invariant mass distributions for both MC and data with a clear peak corresponding to the π^0 signal (see Fig. 17).

A summary of the number of extracted Σ^0 events and the Σ^0/Λ ratio is given in

Table 11
$\Sigma^{\star+} \to \Lambda\pi^+$ *summary*

$N(\Sigma^{\star+})$	full sample	Λ fragmentation region		type of target nucleon	
		$x_F < 0$	$x_F > 0$	νp	νn
DATA	416 ± 80	358 ± 65	63 ± 47	297 ± 61	120 ± 51
MC(meas.)	2070 ± 68	1427 ± 57	649 ± 37	1321 ± 49	754 ± 46
MC(pred.)	1783	1254	529	1150	634
$N(\Sigma^{\star+})/N(\Lambda)$					
DATA (%)	5.2 ± 1.0	6.4 ± 1.2	2.5 ± 1.9	8.6 ± 1.8	2.6 ± 1.1
MC (%)	17.0 ± 0.6	15.9 ± 0.6	20.6 ± 1.2	32.6 ± 1.2	9.3 ± 0.6

Table 12
$\Sigma^{\star-} \to \Lambda\pi^-$ *summary*

$N(\Sigma^{\star-})$	full sample	Λ fragmentation region		type of target nucleon	
		$x_F < 0$	$x_F > 0$	νp	νn
DATA	206 ± 63	121 ± 51	93 ± 37	100 ± 35	111 ± 52
MC(meas.)	551 ± 48	410 ± 42	145 ± 25	18 ± 22	528 ± 43
MC(pred.)	489	362	126	33	456
$N(\Sigma^{\star-})/N(\Lambda)$					
DATA (%)	2.6 ± 0.8	2.2 ± 0.9	3.7 ± 1.5	2.9 ± 1.0	2.4 ± 1.1
MC (%)	4.5 ± 0.4	4.6 ± 0.5	4.6 ± 0.8	0.4 ± 0.5	6.5 ± 0.5

Table 14. For the Σ^0 mass we have taken the value from [34]: m(Σ^0)=1192.6 MeV, while for the width the experimental resolution of 9 MeV has been used. The q_0 value is 74 MeV.

The Σ^0 peak has been fitted by a Gaussian function.

5.3 Yields of strange resonances and heavy hyperons

We compute integral yields of strange resonances and heavy hyperons produced in ν_μ CC using information on the ratios resonance/V^0 and V^0 yields in ν_μ CC MC

Table 13
$\Xi^- \to \Lambda\pi^-$ *summary*

N(Ξ^-)	full sample	Λ fragmentation region		type of target nucleon	
		$x_F < 0$	$x_F > 0$	νp	νn
DATA	42 ± 30	21 ± 24	18 ± 17	54 ± 18	-11 ± 24
MC(meas.)	43 ± 18	33 ± 15	13 ± 9	9 ± 8	36 ± 16
MC(pred.)	60	47	15	14	47
N(Ξ^-)/N(Λ)					
DATA (%)	0.5 ± 0.4	0.4 ± 0.4	0.7 ± 0.7	1.6 ± 0.5	-0.2 ± 0.5
MC (%)	0.4 ± 0.2	0.4 ± 0.2	0.4 ± 0.3	0.2 ± 0.2	0.4 ± 0.2

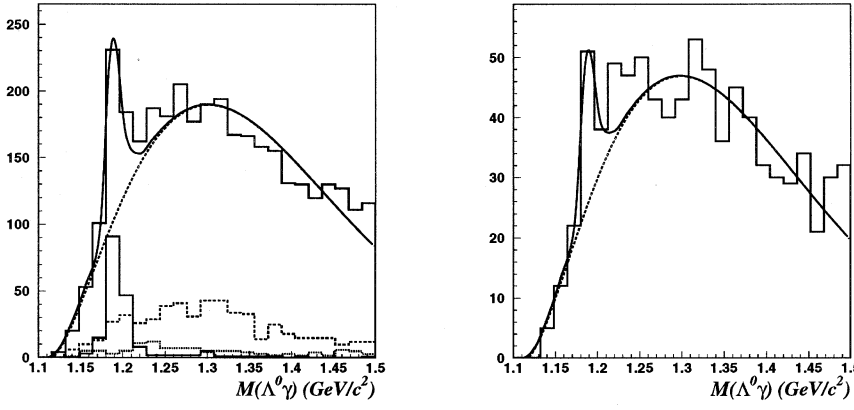

Fig. 16. $\Lambda\gamma$ *invariant mass distributions for both MC (left) and data (right). The MC plot shows the expected signal peak and reflections from* $\Xi^0 \to \Lambda\pi^0$ *and* $\Sigma^{*0} \to \Lambda\pi^0$ *decays.*

events as follows:

$$\left(\frac{N_{res}^{true}}{N_{V^0}^{true}}\right)_{data} = \left(\frac{N_{res}^{rec}}{N_{V^0}^{rec}}\right)_{data} \cdot \left(\frac{N_{res}^{true}}{N_{V^0}^{true}}\right)_{MC} / \left(\frac{N_{res}^{rec}}{N_{V^0}^{rec}}\right)_{MC} \tag{11}$$

The corresponding results are given in Table 15.

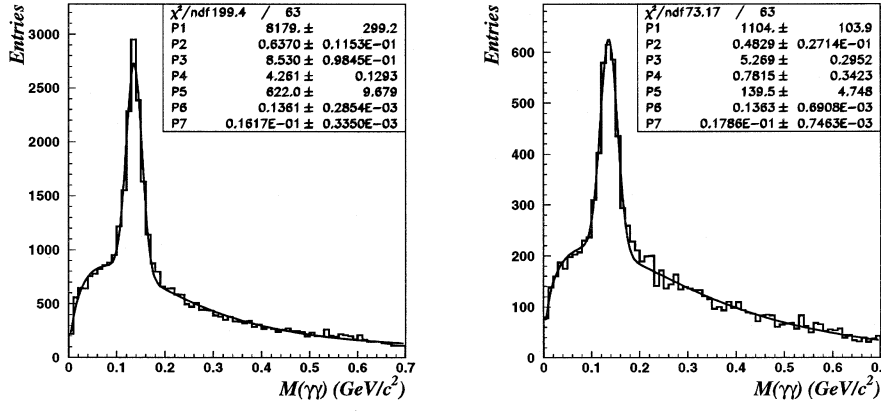

Fig. 17. *$\gamma\gamma$ invariant mass distributions for MC (left) and data (right). Both photons have been reconstructed as conversions in the DC fiducial volume and identified by our V^0 identification procedure. A clear peak corresponding to π^0 signal is visible in both distributions. The parameters P_6 and P_7 show the mass and the width of the Gaussian function after the fit.*

Table 14
$\Sigma^0 \to \Lambda\gamma$ *summary*

N(Σ^0)	full sample	Λ fragmentation region		type of target nucleon	
		$x_F < 0$	$x_F > 0$	νp	νn
DATA	29 ± 10	17 ± 9	16 ± 7	16 ± 7	13 ± 7
MC(meas.)	82 ± 12	50 ± 9	37 ± 8	19 ± 7	61 ± 10
MC(pred.)	80	57	22	22	57
N(Σ^0)/N(Λ)					
DATA (%)	0.4 ± 0.1	0.3 ± 0.2	0.7 ± 0.3	0.5 ± 0.2	0.3 ± 0.2
MC (%)	0.7 ± 0.1	0.6 ± 0.1	1.2 ± 0.3	0.5 ± 0.2	0.8 ± 0.1

5.4 Discussion

The results of our study confirm discrepancies reported earlier [14] in the description of the strange resonances and heavy hyperons production in neutrino interactions by the LUND model with default parameters [25,26]. These results could be potentially used to tune the MC parameters responsible for the fragmentation into strange

Table 15
Corrected yields of strange resonances and heavy hyperons in the data (in %).

yields	$K^{\star+}$	$K^{\star-}$	$\Sigma^{\star+}$	$\Sigma^{\star-}$	Σ^0	Ξ^-
N_{res}/N_{V^0}	15.5 ± 0.9	8.7 ± 0.7	5.8 ± 1.1	2.6 ± 0.8	7.3 ± 2.4	1.9 ± 1.7

particles. Moreover, an additional analysis of events with multiple production of neutral strange particles could be very useful in this respect. Such analysis for ν_μ CC events is currently in progress.

6 CONCLUSION

We reported the results of the study of strange particle production in ν_μ CC interactions using the data from the NOMAD experiment. Our analysis is based on a sample of $\sim 1.3 \times 10^6$ ν_μ CC events, containing 15074 identified K^0_s, 8087 identified Λ and 649 identified $\bar{\Lambda}$ decays. This V^0 sample represents at least a factor of 5 increase in statistics compared to previous (anti)neutrino experiments performed with bubble chambers. Both integral and differential production rates of neutral strange particles (K^0_s, Λ, $\bar{\Lambda}$) have been measured in this analysis. The differential $\bar{\Lambda}$ production rates are measured for the first time in a neutrino experiment. The decay modes of resonances and heavy hyperons with identified V^0's in the final state have been analyzed. Clear signals corresponding to $K^{\star\pm}$, $\Sigma^{\star\pm}$, Ξ^- and Σ^0 have been observed. This study, being potentially interesting for tuning of the Monte Carlo simulation program, is also of special importance for quantitative theoretical interpretation of the Λ and $\bar{\Lambda}$ polarization measurements reported earlier [1,2].

Acknowledgements

We gratefully acknowledge the CERN SPS accelerator and beam-line staff for the magnificent performance of the neutrino beam during the data taking period of the NOMAD experiment.

Our special thanks to all the colleagues from the NOMAD collaboration for their crucial contribution to the analysis presented in this article.

References

[1] P.Astier *et al.*, [NOMAD Collaboration], Nucl. Phys. **B588** (2000) 3

[2] P.Astier *et al.*, [NOMAD Collaboration], Nucl. Phys. **B605** (2001) 3

[3] S.J.Barish *et al.*, Phys. Rev. Lett. **33** (1974) 1446

[4] H.Deden *et al.*, Phys. Lett. **B58** (1975) 361

[5] J.P.Berge *et al.*, Phys. Rev. Lett. **36** (1976) 127

[6] H.Deden *et al.*, Phys. Lett. **B67** (1977) 474

[7] J.P.Berge *et al.*, Phys. Rev. **D18** (1978) 1359

[8] V.Ammosov *et al.*, Nucl. Phys. **B162** (1980) 205

[9] N.J.Baker *et al.*, Phys. Rev. **D24** (1981) 2779

[10] V.Ammosov *et al.*, Nucl. Phys. **B177** (1981) 365

[11] R.Brock *et al.*, Phys. Rev. **D25** (1982) 1753

[12] H.Grässler *et al.*, Nucl. Phys. **B194** (1982) 1

[13] P.Bosetti *et al.*, Nucl. Phys. **B209** (1982) 29

[14] D.Allasia *et al.*, Nucl. Phys. **B224** (1983) 1

[15] C.C.Chang *et al.*, Phys. Rev. **D27** (1983) 2776

[16] D.Allasia *et al.*, Phys. Lett. **B154** (1985) 231

[17] G.T.Jones *et al.*, Z. Phys. **C28** (1985) 23

[18] N.J.Baker *et al.*, Phys. Rev. **D34** (1986) 1251

[19] V.Ammosov *et al.*, Z. Phys. **C30** (1986) 183

[20] S.Willocq *et al.*, Z. Phys. **C53** (1992) 207

[21] G.T.Jones *et al.*, Z. Phys. **C57** (1993) 197

[22] D.DeProspo *et al.*, Phys. Rev. **D50** (1994) 6691

[23] J.Altegoer *et al.*, [NOMAD Collaboration], Nucl. Instr. and Meth. **A404** (1998) 96

[24] J.Altegoer *et al.*, [NOMAD Collaboration], Phys. Lett. **B431** (1998) 219
P.Astier *et al.*, [NOMAD Collaboration], Phys. Lett. **B453** (1999) 169
P.Astier *et al.*, [NOMAD Collaboration], Phys. Lett. **B483** (2000) 387
P.Astier *et al.*, [NOMAD Collaboration], CERN-EP/2001-043, hep-ex/0106102, *to be published in* Nuclear Physics B.

[25] G.Ingelman, LEPTO version 6.1, "The Lund Monte Carlo for Deep Inelastic Lepton-Nucleon Scattering", TSL-ISV-92-0065 (1992)
G.Ingelman, A.Edin, J.Rathsman, LEPTO version 6.5, Comp. Phys. Comm. **101** (1997) 108, [hep-ph/9605286]

[26] T.Sjöstrand, "PYTHIA 5.7 and JETSET 7.4: physics and manual", LU-TP-95-20 (1995), [hep-ph/9508391]
T.Sjöstrand, Comp. Phys. Comm **39** (1986) 347, **43** (1987) 367

[27] GEANT : Detector Description and Simulation Tool, *CERN Programming Library Long Writeup* **W5013**, GEANT version 3.21

[28] M.Glück, E.Reya, A.Vogt, Z. Phys. **C53** (1992) 127

[29] H.Plothow-Besch, Comp. Phys. Comm. **75** (1993) 396

[30] P.Astier *et al.*, [NOMAD Collaboration], "Prediction of neutrino fluxes in the NOMAD experiment", *paper in preparation*

[31] M.Anfreville *et al.*, "The drift chambers of the NOMAD experiment", hep-ex/0104012, *to be published in Nucl. Instr. and Meth.*

[32] D.Autiero *et al.*, Nucl. Instr. and Meth. **A373** (1996) 358;
D.Autiero *et al.*, Nucl. Instr. and Meth. **A387** (1997) 352;
D.Autiero *et al.*, Nucl. Instr. and Meth. **A411** (1998) 285

[33] D.V.Naumov, PhD Thesis, JINR, Dubna, Russia, 2001, *in Russian*

[34] Review of Particle Properties, Eur. Phys. J. **C15** (2000)

[35] G.T.Jones *et al.*, Z. Phys. **C27** (1985) 43

[36] P.D.Acton *et al.*, [OPAL Collaboration], Z. Phys. **C56** (1992) 521

[37] P.Abreu *et al.*, [DELPHI Collaboration], Z. Phys. **C65** (1995) 587

[38] M.R.Adams *et al.*, [E665 Collaboration], Z. Phys. **C61** (1994) 539

[39] M.Derrick *et al.*, [ZEUS Collaboration], Z. Phys. **C68** (1995) 29

[40] S.Aid *et al.*, [H1 Collaboration], Nucl. Phys. **B480** (1996) 3

[41] C.Lachaud, PhD Thesis, Université Denis Diderot (Paris 7), May 2000, *in French*

[42] J.D.Jackson, Nuovo Cimento **34** (1964) 1644

[43] MINUIT package, *CERN Program Library Long Writeup* **D506** (1994)

Received by Publishing Department
on July 11, 2001.

Наумов Д.В., Попов Б.А. E1-2001-139

Исследование рождения странных частиц в ν_μ-взаимодействиях по каналу заряженного тока в эксперименте NOMAD

С использованием уникальных экспериментальных данных, накопленных сотрудничеством NOMAD, выполнено исследование процессов рождения странных частиц в нейтринных взаимодействиях. Анализ ~$1{,}3\times10^6$ взаимодействий ν_μ по каналу заряженного тока с использованием разработанной процедуры идентификации распадов типа V^0 позволил выявить 15074 K^0_s-, 8087 Λ- и 649 $\overline{\Lambda}$-кандидатов. Полученный набор событий более чем в 5 раз превосходит максимальную статистику предшествующих (анти)нейтринных экспериментов на пузырьковых камерах.

Измерены как интегральные, так и дифференциальные выходы нейтральных странных частиц: K^0_s, Λ, $\overline{\Lambda}$. Изучена зависимость дифференциальных выходов от основных кинематических переменных в нейтринном взаимодействии (E_ν, W^2, Q^2) и от поведения частицы внутри адронной струи (x_F, z, p_T^2).

Исследованы возможные моды распадов резонансов и тяжелых гиперонов с образованием нейтральных странных частиц в конечном состоянии. Обнаружены следующие частицы: $K^{*\pm}$, $\Sigma^{*\pm}$, Ξ^- и Σ^0.

Результаты данного исследования важны для теоретической интерпретации измерений поляризации Λ ($\overline{\Lambda}$)-гиперонов, выполненных ранее. Они также представляют интерес для более правильного модельного описания процессов рождения странных частиц в нейтринных взаимодействиях.

Работа выполнена в Лаборатории ядерных проблем им. В.П.Джелепова ОИЯИ.

Сообщение Объединенного института ядерных исследований. Дубна, 2001

Naumov D.V., Popov B.A. E1-2001-139

A Study of Strange Particle Production in ν_μ Charged Current Interactions in the NOMAD Experiment

A study of strange particle production in ν_μ charged current interactions has been performed using the data from the NOMAD experiment. The analysis is based on a sample of ~1.3×10^6 ν_μ CC events, containing 15074 identified K^0_s, 8087 identified Λ and 649 identified $\overline{\Lambda}$ decays. This V^0 sample represents at least a factor of 5 increase in statistics compared to previous (anti)neutrino experiments performed with bubble chambers. Both integral and differential production rates of neutral strange particles (K^0_s, Λ, $\overline{\Lambda}$) have been measured. Mean multiplicities are reported as a function of the event kinematic variables E_ν, W^2 and Q^2 as well as the variables describing particle behaviour in a hadronic jet: x_F, z and p_T^2. The decay modes of resonances and heavy hyperons with identified V^0's (K^0_s, Λ, $\overline{\Lambda}$) in the final state have been analyzed. Clear signals corresponding to $K^{*\pm}$, $\Sigma^{*\pm}$, Ξ^- and Σ^0 have been observed. This study, being potentially interesting for tuning of the Monte Carlo simulation program, is also of special importance for quantitative theoretical interpretation of the Λ and $\overline{\Lambda}$ polarization measurements reported earlier.

The investigation has been performed at the Dzhelepov Laboratory of Nuclear Problems, JINR.

Communication of the Joint Institute for Nuclear Research. Dubna, 2001

Макет Т.Е.Попеко

Подписано в печать 24.07.2001
Формат 60 × 90/16. Офсетная печать. Уч.-изд. л. 3,5
Тираж 375. Заказ 52795. Цена 4 р. 20 к.

Издательский отдел Объединенного института ядерных исследований
Дубна Московской области